Improved Distinction by MR Spectroscopy of Suspicious Lesions after Radiation Therapy among Children with Primary Brain Tumors

Karen Belkić & Dževad Belkić

Department of Oncology-Pathology, Karolinska Institutet

- **Brain tumors are the leading cause of cancer-related deaths among children.**
- **Radiation therapy (RT) is indicated for unresectable and/or malignant brain tumors.**
- **After RT, primary brain tumors frequently recur.**
- **Changes in brain tissue can also be provoked by RT, and these are difficult to distinguish from recurrent tumor using magnetic resonance imaging (MRI).**

Increasing attention in pediatric neuro-oncology has been given to magnetic resonance spectroscopy (MRS) and spectroscopic imaging (MRSI).

We systematically examine MRS and MRSI data concerning distinction of

Recurrent brain tumor

versus

Radiation necrosis post-RT

among children with primary brain tumors.

Table 1 Pediatric patients with recurrent tumor versus radiation necrosis post-RT for primary malignant brain tumors examined by MRS or MRSI

1st Author, publication y [reference #] center country	Study description MR data acquisition	The pediatric patient(s)	MRS Data	Clinical outcome of the pediatric patient(s)
Kamada, [41] Hokkaido U, Sapporo, Japan	A series of 10 patients with 1° brain tumors. B_0 = 1.5T, TE=270 ms Single voxel MRS -- VOI selected to contain the bulk of the lesion but avoid overlapping with bone marrow and surrounding brain tissue.	Age 7 with glioblastoma treated surgically and with RT (65 Gy). MRS performed 8 M after RT (Gender not indicated)	Cho/Cr = 3.00 NAA/Cr = 0.00 Lac/Cr = 1.80 Lac/Cho = 0.60	Recurrent tumor The patient underwent repeat surgery and died of locally recurrent tumor.
Nakajima, [43] Tohoku U, Sendai, Japan	A series 18 patients with histologically-confirmed glioma who after RT+ Chemotx had a subsequent lesion on MRI suspected to be tumor recurrence versus RN from CE & T_2 B_0 =1.5T, TE= 272 MRS of representative part of the CE lesion. Retrospective analysis of patients who had been followed every 2-3 M, up to 158 M	Age 14, female with diffuse astrocytoma, received RT (60 Gy) and Chemotx. MRS performed 80 M post RT.	Cho/Cr = 2.21 Lac/Cho = 0.43	Recurrent tumor The patient died of tumor progression to anaplastic astrocytoma histologically confirmed, 96 months after RT.
Weybright, [42] Smith, [44] Elias [45] U Michigan, Ann Arbor, USA	A series of 33 patients with primary brain tumor grade II-IV histopathologically proven, previous conventional fractionated 54-70 Gy RT with or without Chemotx and, subsequently, a new CE-lesion in the location of the RT. B_0 = 1.5T, TE=144 ms, MRSI performed in all cases, the voxel chosen was that with the most abnormal spectra In four patients a second set of MRS data is reported [45] and included in the table.	Age 7, male with ependymoma Followed for 22 M	Cho/Cr = 3.24 NAA/Cr = 1.01 Cho/NAA = 3.21 --- Cho/Cr = 2.57 NAA/Cr = 1.14 Cho/NAA = 2.25	Recurrent tumor histologically confirmed
		Age 4, male with medullary glioma Followed for 21 M	Cho/Cr = 2.79 NAA/Cr = 1.13 Cho/NAA = 2.47 --- Cho/Cr = 3.87 NAA/Cr = 2.07 Cho/NAA = 1.87	Recurrent tumor Based on imaging and clinical course
		Age 17, male with medullary glioma Followed for 24 M	Cho/Cr = 4.26 NAA/Cr = 0.62 Cho/NAA = 6.19	Recurrent tumor Based on imaging and clinical course
		Age 14, male with medulloblastoma Followed for 22 M	Cho/Cr = 1.69 NAA/Cr = 0.90 Cho/NAA = 1.88	Radiation necrosis Based on imaging and clinical course
		Age 17, female with medulloblastoma Followed for 22 M	Cho/Cr = 1.61 NAA/Cr = 0.94 Cho/NAA = 1.71	Radiation necrosis Absence of tumor confirmed by biopsy
		Age 10, female with oligoastrocytoma Followed for 11 M	Cho/Cr = 0.72 NAA/Cr = 0.93 Cho/NAA = 0.83 --- Cho/Cr = 1.22 NAA/Cr = 1.17 Cho/NAA = 1.05	Radiation necrosis assessed by imaging
		Age 7, female with primitive neuroectodermal tumor Followed for 20 M	Cho/Cr = 1.58 NAA/Cr = 1.28 Cho/NAA = 1.23 --- Cho/Cr = 0.86 NAA/Cr = 0.98 Cho/NAA = 0.88	Radiation necrosis assessed by imaging

Abbreviations: CE = contrast enhancement, Chemotx = chemotherapy, Cho = choline, Cr = creatine, Gy = Gray, Lac = lactate, M = months MRS = magnetic resonance spectroscopy MRSI = magnetic resonance spectroscopic imaging ms = milliseconds NAA = n-acetyl aspartate RT = radiation therapy T = tesla TE = echo time, Tx = therapy or treated, U = university VOI = voxel of interest

Table 2 Comparison of metabolites ratios assessed via magnetic resonance spectroscopy among pediatric patients with recurrent brain tumor versus radiation necrosis

	Recurrent Tumor		Radiation Necrosis
	Mean ± sd (Range)	Significance	Mean ± sd (Range)
Choline to creatine	3.13 ± 0.72 (2.21 - 4.26)	**	1.28 ± 0.41 (0.72 – 1.69)
Choline to N-acetyl aspartate	3.20 ± 1.74 (1.87 – 6.19)	*	1.26 ± 0.44 (0.83 – 1.88)
N-acetyl aspartate to creatine	1.0 ± 0.68 (0.00 – 2.07)	NS	1.03 ± 0.15 (0.90 – 1.28)

Differences between tumor recurrence versus radiation necrosis were assessed by the Mann-Whitney test.

* and ** denote $p < 0.05$ and $p < 0.01$, respectively, NS denotes not statistically significant ($p \geq 0.05$)

Based upon reported data from Refs. [41-45]

- From the limited available data, it appears that, among children:

- Choline-to-creatine > 2 indicate tumor recurrence

whereas

- Choline-to-creatine ratios < 2 are associated with radiation necrosis.

- More extensive analysis of the adult plus pediatric population, however, has indicated that, while helpful, metabolite ratios do not provide unequivocal distinction between recurrent tumor and radiation necrosis.

These limitations are likely related to reliance upon sub-optimal signal processing methods conventionally used within MRS and MRSI.

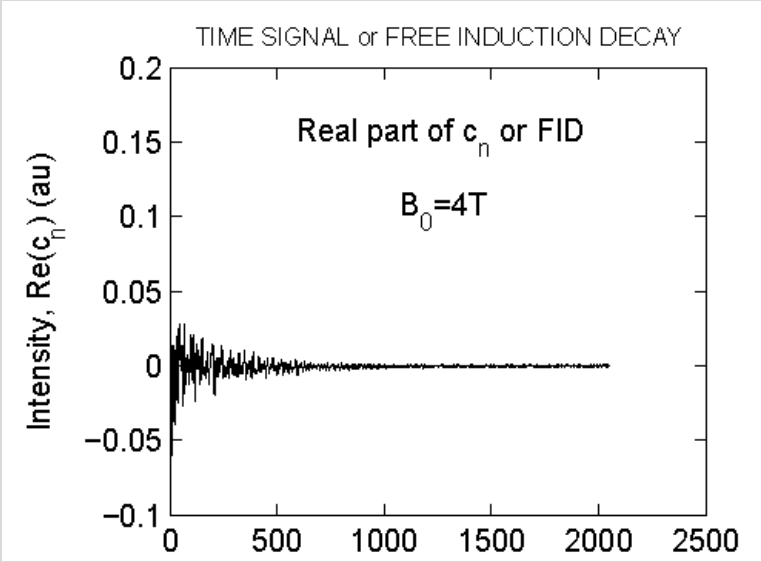

- An MR time signal as encoded in vivo at 4T from healthy human occipital grey matter.
- This is a complex-valued time signal, with the real part shown herein. Each time signal point is divided by 2048 x 102.

Currently, the fast Fourier transform is used in clinical MR scanners.

The Fourier spectrum is given by:

$$F_k = \frac{1}{N}\sum_{n=0}^{N-1} c_n \, e^{-2i\pi kn/N} \quad 1 \le k \le N-1$$

where $2\pi k/T$ are the fixed Fourier grid frequencies , unrelated to the actual resonances frequencies ω_k .

T is the total acquisition time $T = N/\tau$ and τ is the sampling time and c_n are the time signal points.

The Fast Fourier Transform (FFT)

Gives the spectrum as a single polynomial

- **Non-parametric: Supplies only a total shape spectrum**
- **Quantification via FITTING (post-processing): NON-UNIQUE**
- **Number of metabolites guessed *prior* to fitting**

  This may ⇒ false peaks (over-fitting), as well as undetected true metabolites (under-fitting)

$F(\omega_k)$ with pre-assigned angular frequencies, ω_k

whose minimal separation $\omega_{\min} = 2\pi k / T$

is determined by the epoch T

The FFT spectrum is defined

only on the Fourier grid points

$$\omega_k = \pm k/T$$

where $(k = 0,1,2,3\ldots N-1)$

and N is the signal length.

- **Low resolution**
- **Linearity: imports noise as intact from measured time domain data**

Among the advanced
signal processing methods,
the fast Padé transform (FPT)
is particularly suitable
for improving the diagnostic yield
of *in vivo* MRS

Belkić Dž, *Quantum Mechanical Signal Processing and Spectral Analysis*, Institute of Physics Publishing, Bristol, 2004.

Belkić K, Molecular Imaging through Magnetic Resonance for Clinical Oncology, Cambridge International Science Publishing, Cambridge, 2004.

Belkić Dž, Belkić K, *Signal Processing in Magnetic Resonance Spectroscopy with Biomedical Applications, Taylor & Francis Publishers,* London, 2010.

THE FAST PADÉ TRANSFORM (FPT)

A non-linear, rational polynomial as the Padé approximant to the exact spectrum of the encoded time signal points.

Extracts diagnostically important quantitative information, otherwise unavailable in full depth using conventional estimators for *in vivo* MRS

The FPT represents the exact spectrum in variable $z^{-1} = e^{-i\omega\tau}$:

$$G(z^{-1}) = (1/N)\sum_{n=0}^{N-1} c_n z^{-n}$$

[1]

by the UNIQUE ratio of two polynomials
e.g. in the diagonal form:

$$G(z^{-1}) \approx P_K(z^{-1}) / Q_K(z^{-1})$$

The FPT

Extrapolation

Interpolation

- Does not use the fixed Fourier mesh ω_k , can be computed at any sweep frequency ω.
- Resolution $\Delta\omega_a$ is not pre-determined by the acquisition time T.

  Resolution is the average distance $\Delta\omega_a$, between adjacent frequencies in a selected range. In a given frequency window, $\Delta\omega_a$ is often smaller than $\Delta\omega_{min}$, thus better resolving power of FPT, relative to FFT.

The resolution of $1/T$ of the FFT is limited by a sharp cut-off

of the time signal $c(t)$ at $t = T$.

The FPT extrapolates $c(t)$ beyond the total acquisition time ($t > T$). This yields a resolution better than $2\pi/T$. The implicit infinite sum from

$$P/Q \equiv PQ^{-1}$$

is contained in the inverse polynomial

$$Q^{-1}$$

Non-linearity, as a ratio: extra degree of freedom to cancel out noise

THE CONUNDRUM BETWEEN INCREASING ACQUISITION TIME FOR IMPROVED RESOLUTION AND INCREASING NOISE IS OBVIATED.

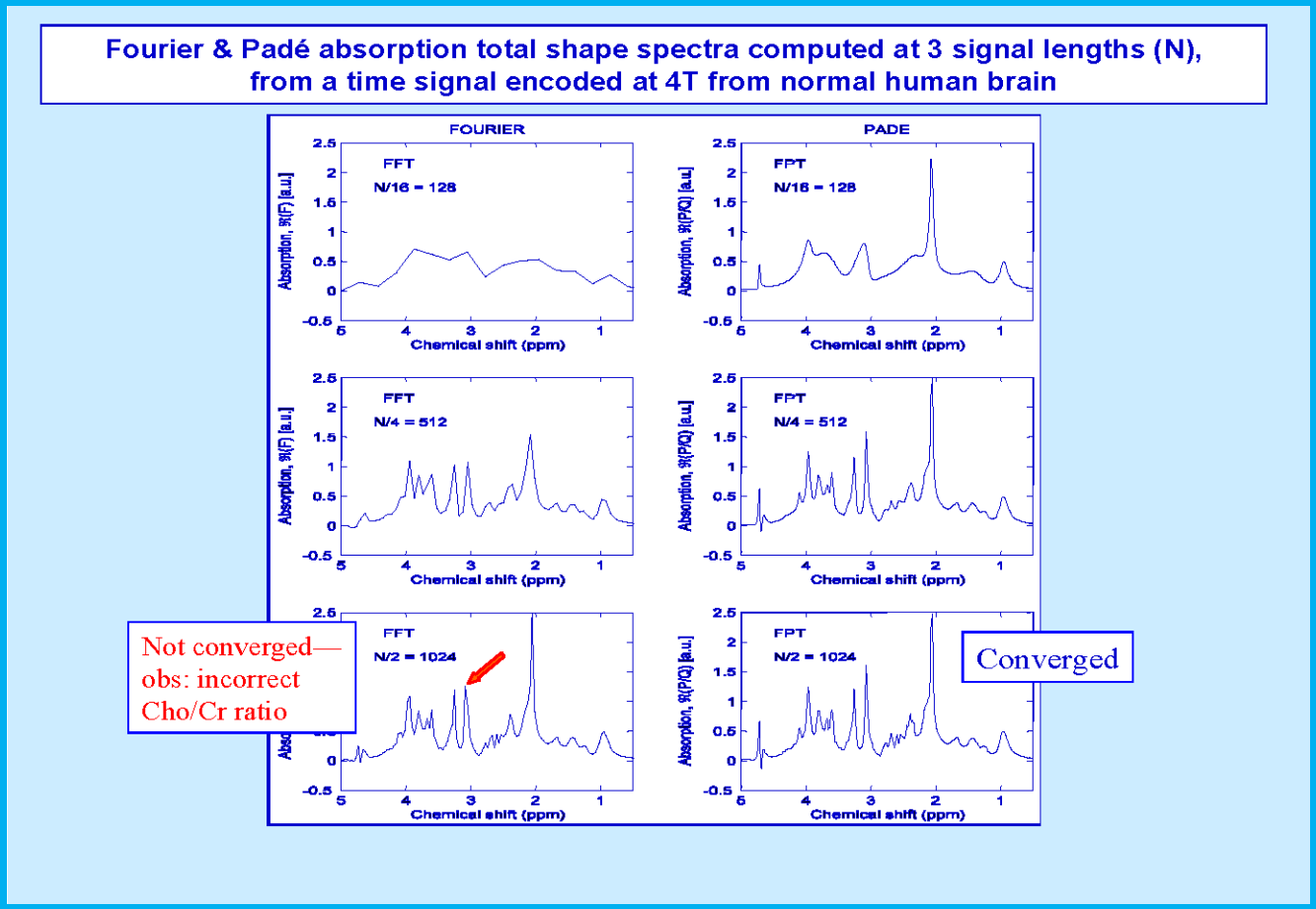

Fourier and Padé absorption spectra computed using an *in vivo* time signal at three partial signal lengths (*N*/16 = 128, *N*/4 = 512, *N*/2 = 1024), where the full signal length is *N* = 2048. The arrow in the bottom left panel points to the choline to creatine ration which, even in the FFT is still incorrect, even at half signal length. The abscissae are chemical shifts, as the relative dimensionless frequencies in part per million (ppm), and the ordinates are intensities in arbitrary units (au). Magnetic field strength: 4T.

The Parametric FPT

- The coefficients of the polynomials $P_K(z^{-1})$ and $Q_K(z^{-1})$ from equation 1 are computed by solving the systems of linear equations.
- The product in $G_N(z^{-1}) * Q_K(z^{-1}) = P_K(z^{-1})$ can be handled as a convolution.
- The characteristic equation $Q_K(z^{-1}) = 0$ is solved to extract the peak parameters $\{\omega_k\}$ and $\{d_k\}$ for each resonance.

This leads to ***K*** unique roots ${z_k}^{-1}$ ($1 \leq k \leq K$), so that the sought eigenfrequency ω_k is deduced

via $\omega_k = (1/\tau) \ln ({z_{k,Q}}^{-1})$.

The FPT extracts the parameters $\{\omega_k, d_k\}$ ($1 \le k \le K$) directly from the raw encoded MRS time signal.

The metabolite concentrations can then be computed from the peak heights and FWHM.

FWHM = full width at half maximum

Peak #	Position	Width	|Amplitude|
1	0.985	0.180	0.122
2	1.112	0.257	0.161
3	1.548	0.172	0.135
4	1.689	0.118	0.034
5	1.959	0.062	0.056
6	2.065	0.031	0.171
7	2.145	0.050	0.116
8	2.261	0.062	0.092
9	2.411	0.062	0.085
10	2.519	0.036	0.037
11	2.675	0.033	0.008
12	2.676	0.062	0.063
13	2.855	0.016	0.005
14	3.009	0.064	0.065
15	3.067	0.036	0.101
16	3.239	0.050	0.096
17	3.301	0.064	0.065
18	3.481	0.031	0.011
19	3.584	0.028	0.036
20	3.894	0.036	0.041
21	3.803	0.024	0.031
22	3.944	0.042	0.068
23	3.965	0.062	0.013
24	4.271	0.055	0.016
25	4.680	0.108	0.057

(i) N_P=256: Position (ppm), Width (ppm), |Amplitude| (au)

Peak #	Chem. Sh.	Relax. t.	Concentr.	Fraction	Metabol.
1	0.985	0.087	7.930	0.71	Lip
2	1.112	0.061	10.46	0.94	Lip
3	1.548	0.091	8.775	0.79	Lip
4	1.689	0.133	2.210	0.20	Lip
5	1.959	0.253	3.640	0.33	Gaba
6	2.065	0.505	11.12	1.00	NAA
7	2.145	0.313	7.540	0.68	NAAG
8	2.261	0.253	5.980	0.54	Gaba
9	2.411	0.253	5.525	0.50	Glu
10	2.519	0.435	2.405	0.22	Gln
11	2.675	0.474	0.520	0.05	Asp
12	2.676	0.253	4.095	0.37	NAA
13	2.855	0.979	0.325	0.03	Asp
14	3.009	0.245	4.225	0.38	Cr
15	3.067	0.435	6.565	0.59	PCr
16	3.239	0.313	6.240	0.56	Cho
17	3.301	0.245	4.225	0.38	PCho
18	3.481	0.505	0.715	0.06	Tau
19	3.584	0.559	2.340	0.21	m-Ins
20	3.894	0.435	2.665	0.24	Glu
21	3.803	0.652	2.015	0.18	Gln
22	3.944	0.373	4.420	0.40	Cr
23	3.965	0.253	0.845	0.08	PCr
24	4.271	0.285	1.040	0.09	PCho
25	4.680	0.145	3.705	0.33	Water

(iv) N_P=256: Ch. Sh. (ppm), Relax. T_2 (s), Conc. (mM/g ww)

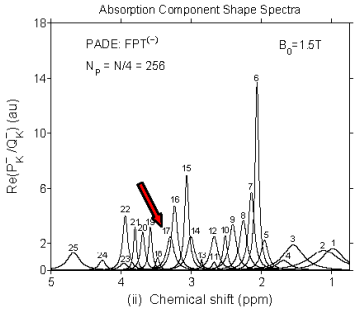

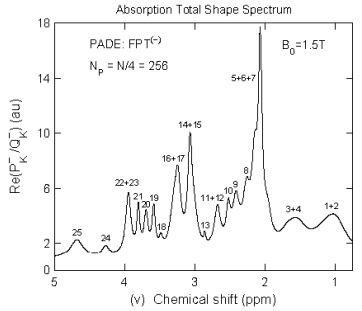

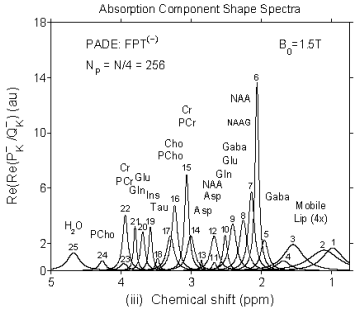

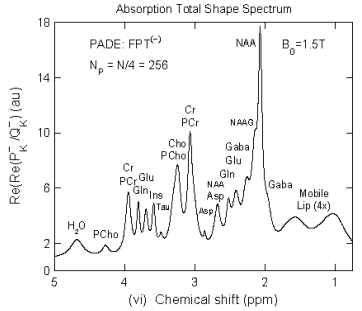

Reconstruction by the fast Padé transform of spectral peak parameters [panel (i)] and metabolite concentrations [panel (iv)] and absorption component [panels (ii), (iii)] and total [panels (v), (vi)] shape spectra for a time signal as encoded clinically from healthy human brain via MRS at $B0$ =1.5T, TE = 20 ms, full length N = 1024, bandwidth 1000 Hz and τ = 1 ms. The arrow at panel (ii) points to peak #17 phosphocholine which underlies choline, peak #16. These two resonances can only be discerned on the component shape spectra (panels (ii) or (iii)) but not on the total shape spectra (panels (v) or (vi)). See list of abbreviations for the metabolite assignments.

Conclusions

Optimized signal processing via the fast Padé transform not only yields accurate metabolite ratios with very high resolution, but also provides reliable quantification of over 20 brain metabolites.

Padé-optimized MRS and MRSI could thereby facilitate differential diagnosis of new lesions appearing on MRI among children treated for primary brain tumors.

These advantages of the fast Padé transform are more broadly applicable to MRS and MRSI within pediatric neuro-oncology and beyond.